Letters

On the Effects of Reflected Waves in Transient Shear Wave Elastography

Thomas Deffieux, Jean-Luc Gennisson, Jeremy Bercoff, and Mickael Tanter

***Abstract*—In recent years, novel quantitative techniques have been developed to provide noninvasive and quantitative stiffness images based on shear wave propagation. Using radiation force and ultrafast ultrasound imaging, the supersonic shear imaging technique allows one to remotely generate and follow a transient plane shear wave propagating *in vivo* in real time. The tissue shear modulus, i.e., its stiffness, can then be estimated from the shear wave local velocity. However, because the local shear wave velocity is estimated using a time-of-flight approach, reflected shear waves can cause artifacts in the estimated shear velocity because the incident and reflected waves propagate in opposite directions. Such effects have been reported in the literature as a potential drawback of elastography techniques based on shear wave speed, particularly in the case of high stiffness contrasts, such as in atherosclerotic plaque or stiff lesions. In this letter, we present our implementation of a simple directional filter, previously used for magnetic resonance elastography, which separates the forward- and backward-propagating waves to solve this problem. Such a directional filter could be applied to many elastography techniques based on the local estimation of shear wave speed propagation, such as acoustic radiation force imaging (ARFI), shearwave dispersion ultrasound vibrometry (SDUV), needle-based elastography, harmonic motion imaging, or crawling waves when the local propagation direction is known and high-resolution spatial and temporal data are acquired.**

Based on the propagation of mechanical shear waves in tissue, quantitative elastography techniques [1]–[6] are able to noninvasively and quantitatively estimate the shear modulus of tissues, i.e., their stiffness. Because palpation is so important as a diagnosis tool, which is emphasized by its dominant role in breast cancer screening, these methods are regarded as highly promising. They are already being clinically tested at different stages for breast cancer detection [7], [8], liver fibrosis staging [2], [9]–[11], kidney monitoring [12], thyroid gland [13] and prostate cancer detection [3], [14], musculoskeletal monitoring [15], [16], and ophthalmologic [17] or vascular applications [18], [19].

In supersonic shear imaging, a transient plane shear wave is generated remotely *in situ* using acoustic radiation force [1]. The shear wave is then acquired, while propagating and in real time, using ultrafast ultrasound imaging (up to 20 kHz) [20]. Based on the shear wave propagation movie, it is then possible to estimate, pixel by pixel, the local shear group velocity, v_g, of the transient plane wave using a time-of-flight approach [21]. Using time-domain cross correlation, the time-of-flight approach allows estimation of the time delay of the shear wave between adjacent points to estimate the local shear wave group velocity, v_g. By estimating this velocity, it is possible to estimate the shear modulus μ either using the well-known equation $\mu = \rho \cdot {v_g}^2$ for quasi homogeneous media, where ρ is the density and v_g the estimated shear wave velocity group, or the full dispersion relation in guided media such as thin layers or tubes (for example, for the cornea [17] or arteries [18]).

Unfortunately, estimating the local shear wave velocity with this time-of-flight approach can yield artifacts if incident and reflected shear waves are present simultaneously, which can be the case when there is a high elastic contrast in the image [22], [23]. Those artifacts can be complex to understand when multiple elastic reconstructions are combined to form a single elasticity image.

Based on the spatio-temporal directional filter proposed by Manduca *et al.* [24], which was applied to magnetic resonance elastography, we present here an implementation of a directional filter for ultrasound-based shear wave elastography and its associated results. This filter, which was introduced several years ago in our reconstruction algorithms, yields strong improvements on the reconstruction quality by separating the incident and reflected propagating shear waves. Because the wave is assumed to be locally planar, it can be written, for a low dispersive and locally homogeneous medium, as the sum of one-dimensional forward- and backward-propagating waves (respectively, U_i and U_r) traveling with a velocity c:

$$\begin{aligned} U(x,t) &= \iint (U_i(\omega)e^{j(\omega t - kx)} + U_r(\omega)e^{j(\omega t + kx)})\mathrm{d}\omega\mathrm{d}k \\ &= \int U_i(\omega)e^{j(\omega t - (\omega x)/c)} + U_r(\omega)e^{j(\omega t + (\omega x)/c)}\mathrm{d}\omega. \end{aligned} \quad (1)$$

By looking at the k-space representation $[k,\omega]$ of a propagating plane wave (1), the domain can easily be separated in four quadrants, $k > 0$ and $\omega > 0$, $k < 0$ and $\omega < 0$, $k < 0$ and $\omega > 0$, and finally $k > 0$ and $\omega < 0$. Depending on the sign of the phase velocity $c = \omega/k$, one can separate the forward ($c > 0$) and backward ($c < 0$) components of a wave by simply multiplying the k-space data by a mask. By smoothly apodizing the borders of this mask to avoid brutal cuts in the spectrum and subsequent Gibbs oscillations in the $[x,t]$ domain, it is possible to design a very simple, yet efficient, directional filter that can entirely remove the reflected components of a propagating wave without any artifacts. This filter operates on each

Manuscript received April 15, 2011; accepted June 28, 2011. This work was partly supported by the French National Agency for Research on AIDS and Viral Hepatitis (ANRS).

T. Deffieux, J.-L. Gennisson, and M. Tanter are with the Institut Langevin, Ondes et Images, École Supérieure de Physique et de Chimie Industrielles de la Ville de Paris ParisTech, Centre National de la Recherche Scientifique UMR 7587, Institut National de la Santé et de la Recherche Médicale U979, Paris, France (e-mail: tdeffieux@gmail.com).

J. Bercoff is with Supersonic Imagine, Aix en Provence, France.

Digital Object Identifier 10.1109/TUFFC.2011.2052

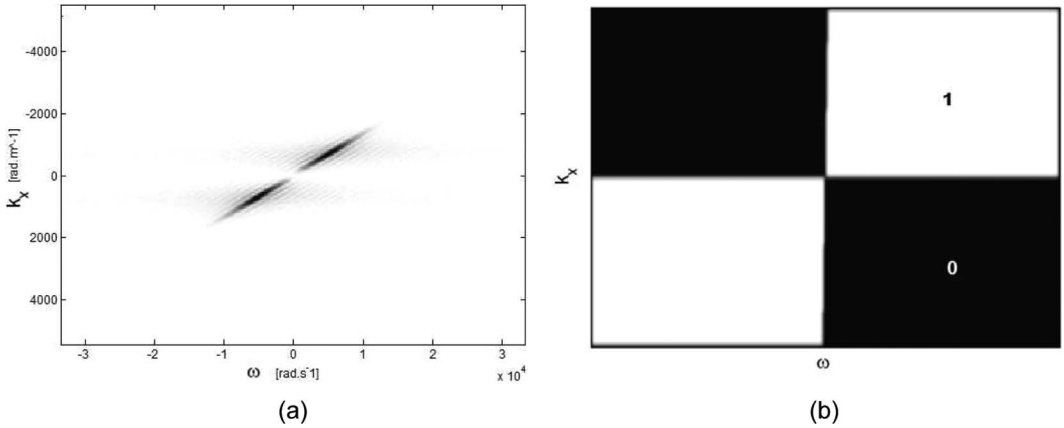

Fig. 1. (a) K-space representation of a propagating plane and transient shear wave (2-D Fourier transform for a given depth). Simulated data of wideband plane shear wave. (b) Coefficients of the filter in the Fourier plane $[k_x, \omega]$. The filter is apodized on the edges to prevent oscillations; its center corresponds to the zero frequencies. The filter is applied using the 2-D fast Fourier transform (FFT) on each depth line of the shear wave propagation movies.

depth line and its design is shown in Fig. 1; the results on experimental and simulated data sets (10-mm spherical inclusion of stiffness 10 kPa in a 5-kPa background) are presented in Fig. 2.

Using elastic finite-difference time-domain numerical simulations [25] of the shear wave propagation (visible in Fig. 2) and *in vitro* elastic phantom experiments, we can illustrate the effects of the directional filter on the shear modulus images (results presented in Figs. 3 and 4).

Reconstruction of shear modulus maps from simulated shear wave propagation movies (finite-difference time-domain elastic solver) are presented in Fig. 3 with and without the directional filter. Different elastic inclusion diameters (8 and 12 mm) and stiffness (10, 15, and 20 kPa) are used to illustrate the efficiency of the filter in different situations.

Fig. 4 presents results obtained in breast elastic phantoms for 3 different inclusions. As shown with simulated data, the effect of the directional filter is quite important. White arrows indicate the artifact positions without the directional filter.

Such a filter, which is easy to implement and fast, can drastically improve the reconstructed shear modulus in stiff inclusions, as seen in Figs. 3 and 4. It can be applied in real time and has always been activated by default for all supersonic shear wave propagation data and associated results. A movie of the shear wave propagation with high spatial and temporal resolution (such as that provided by ultrafast imaging [1]) is required to compute the 2-D Fourier transform accurately and apply this filter.

The proposed filter can also be used to improve the signal-to-noise ratio of the acquired data. By removing nearly half of the k-space domain in which nearly no useful signal is present but where half of the white noise energy is distributed, the filter can significantly improve the signal-to-noise ratio of an acquisition by up to 2-fold.

In conclusion, although reflected shear waves might be rapidly attenuated with larger viscosity, especially *in vivo*, a directional filter is often required in transient shear wave

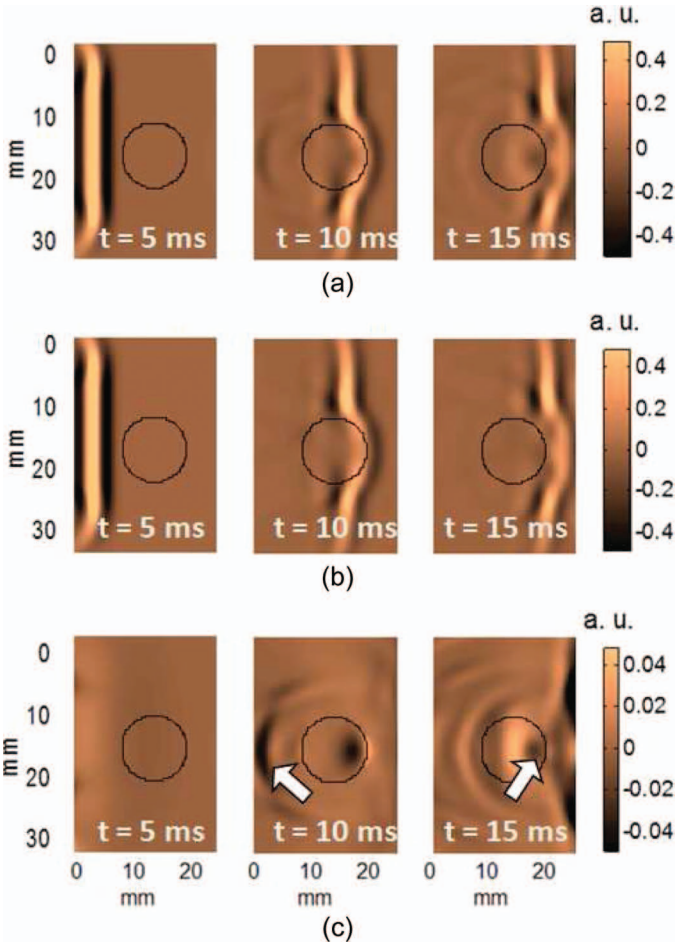

Fig. 2. Simulated shear waves propagating through a 3-D spherical inclusion in arbitrary units (a.u.): (a) unfiltered waves, (b) incident shear wave as separated by the directional filter, (c) reflected shear wave as separated by the directional filter (scale ×10). Here, the reflected wave amplitude is one-tenth of the incident wave but still has an impact on the reconstructed shear modulus value (cf. Fig. 3). The black circle denotes the position of the spherical inclusion.

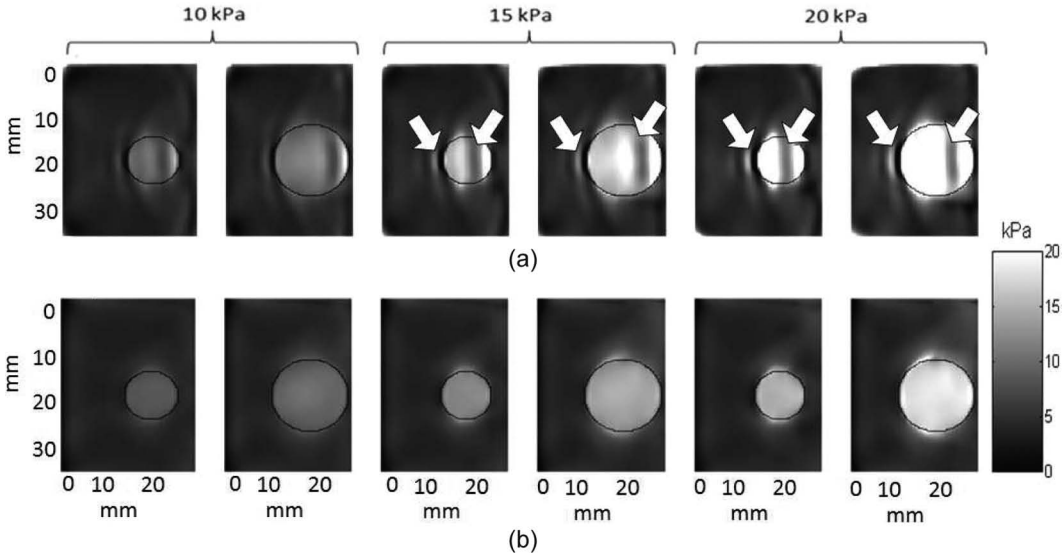

Fig. 3. Shear modulus maps from simulated shear wave propagation data in elastic inclusions of various diameters (8 and 12 mm) and stiffnesses (10, 15, and 20 kPa). (a) Without the directional filter, artifacts are visible in the inclusions with a characteristic overestimation on the edges and an underestimation in the center of the inclusions, as can be observed in experiments (Fig. 4). This pattern is due to interferences between the incident and reflected shear waves. (b) With the directional filter, the artifacts are completely removed.

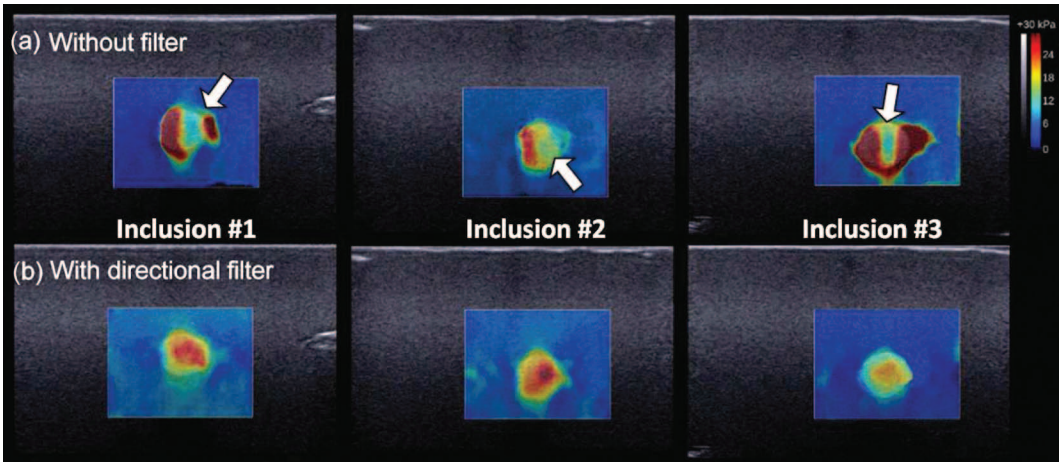

Fig. 4. Shear modulus maps from experimental data acquired on a breast phantom on 3 different inclusions. (a) Without the directional filter, artifacts caused by the reflected shear waves are visible inside the inclusions (white arrows). b) With the directional filter, those artifacts are greatly reduced. Background shear modulus is 5 kPa and inclusions' stiffnesses are between 15 and 20 kPa.

elastography to prevent bias from appearing in the local shear velocity estimation. By separating the forward and backward components, it is possible to almost entirely remove the reflected wave and reduce those artifacts in the shear modulus maps of a stiff inclusion. In practice, and for all clinical applications, such a simple filter is always used by default to improve image quality. It is highly recommended in transient shear wave applications [2]–[6], [26] to avoid reflection artifacts.

References

[1] J. Bercoff, M. Tanter, and M. Fink, "Supersonic shear imaging: A new technique for soft tissue elasticity mapping," *IEEE Trans. Ultrason. Ferroelectr. Freq. Control*, vol. 51, pp. 396–409, 2004.

[2] M. L. Palmeri, M. H. Wang, J. J. Dahl, K. D. Frinkley, and K. R. Nightingale, "Quantifying hepatic shear modulus in vivo using acoustic radiation force," *Ultrasound Med. Biol.*, vol. 34, pp. 546–558, 2008.

[3] F. G. Mitri, M. W. Urban, M. Fatemi, and J. F. Greenleaf, "Shear wave dispersion ultrasonic vibrometry for measuring prostate shear stiffness and viscosity: An in vitro pilot study," *IEEE Trans. Biomed. Eng.*, vol. 58, no. 2, pp. 235–242, Feb. 2011.

[4] M. Orescanin, M. A. Qayyum, K. S. Toohey, and M. F. Insana, "Dispersion and shear modulus measurements of porcine liver," *Ultrason. Imaging*, vol. 32, no. 4, pp. 255–266, Oct. 2010.

[5] J. Vappou, C. Maleke, and E. E. Konofagou, "Quantitative viscoelastic parameters measured by harmonic motion imaging," *Phys. Med. Biol.*, vol. 54, no. 11, pp. 3579–3594, Jun. 2009.

[6] Z. Hah, C. Hazard, Y. T. Cho, D. Rubens, and K. Parker, "Crawling waves from radiation force excitation," *Ultrason. Imaging*, vol. 32, no. 3, pp. 177–189, Jul. 2010.

[7] A. Athanasiou, A. Tardivon, M. Tanter, B. Sigal-Zafrani, J. Bercoff, T. Deffieux, J.-L. Gennisson, M. Fink, and S. Neuenschwander, "Breast lesions: Quantitative elastography with supersonic shear im-

aging—Preliminary results," *Radiology*, vol. 256, no. 1, pp. 297–303, Jul. 2010.

[8] R. Sinkus, M. Tanter, T. Xydeas, and S. Catheline, "Viscoelastic shear properties of in vivo breast lesions measured by MR elastography," *Magn. Reson. Imaging*, vol. 23, no. 2, pp. 159–165, 2005.

[9] L. Castéra, J. Vergniol, J. Foucher, and B. L. Bail, "Prospective comparison of transient elastography, FibrotTest, APRI, and liver biopsy for the assessment of fibrosis in chronic hepatitis C," *Gastroenterology*, vol. 128, no. 2, pp. 343–350, 2005.

[10] L. Huwart, C. Sempoux, E. Vicaut, N. Salameh, L. Annet, E. Danse, F. Peeters, L. ter Beek, J. Rahier, and R. Sinkus, "Magnetic resonance elastography for the noninvasive staging of liver fibrosis," *Gastroenterology*, vol. 135, no. 1, pp. 32–40, 2008.

[11] M. Muller, J.-L. Gennisson, T. Deffieux, M. Tanter, and M. Fink, "Quantitative viscoelasticity mapping of human liver using supersonic shear imaging: Preliminary in vivo feasibility study," *Ultrasound Med. Biol.*, vol. 35, no. 2, pp. 219–229, Feb. 2009.

[12] J. L. Gennisson, N. Grenier, R. Hubrecht, L. Couzy, Y. Delmas, M. Derieppe, S. Lepreux, P. Merville, A. Criton, J. Bercoff, and M. Tanter, "Multiwave technology introducing shear wave elastography of the kidney: Pre-clinical study on a kidney fibrosis model and clinical feasibility study on 49 human renal transplants.," in *Proc. IEEE Ultrasonic Symp.*, San Diego, CA, 2010.

[13] F. Sebag, J. Vaillant-Lombard, J. Berbis, V. Griset, J. F. Henry, P. Petit, and C. Oliver, "Shear wave elastography: A new ultrasound imaging mode for the differential diagnosis of benign and malignant thyroid nodules," *J. Clin. Endocrinol. Metab.*, vol. 95, no. 12, pp. 5281–5288, Sep. 2010.

[14] R. Chopra, A. Arani, Y. Huang, M. Musquera, J. Wachsmuth, M. Bronskill, and D. Plewes, "In vivo MR elastography of the prostate gland using a transurethral actuator," *Magn. Reson. Med.*, vol. 62, no. 3, pp. 665–671, Sep. 2009.

[15] J. Basford, T. Jenkyn, K. An, R. Ehman, G. Heers, and K. Kaufman, "Evaluation of healthy and diseased muscle with magnetic resonance elastography," *Arch. Phys. Med. Rehabil.*, vol. 83, no. 11, pp. 1530–1536, Nov. 2002.

[16] J.-L. Gennisson, T. Deffieux, E. Macé, G. Montaldo, M. Fink, and M. Tanter, "Viscoelastic and anisotropic mechanical properties of in vivo muscle tissue assessed by supersonic shear imaging," *Ultrasound Med. Biol.*, vol. 36, no. 5, pp. 789–801, May 2010.

[17] M. Tanter, D. Touboul, J. L. Gennisson, J. Bercoff, and M. Fink, "High-resolution quantitative imaging of cornea elasticity using supersonic shear imaging," *IEEE Trans. Med. Imaging*, vol. 28, no. 12, pp. 1881–1893, 2009.

[18] M. Couade, M. Pernot, C. Prada, E. Messas, J. Emmerich, P. Bruneval, A. Criton, M. Fink, and M. Tanter, "Quantitative assessment of arterial wall biomechanical properties using shear wave imaging," *Ultrasound Med. Biol.*, vol. 36, no. 10, pp. 1662–1676, Oct. 2010.

[19] M. Couade, M. Pernot, E. Messas, A. Bel, M. Ba, H. Albert, M. Fink, and M. Tanter, "In vivo quantitative mapping of myocardial stiffening and transmural anisotropy during the cardiac cycle," *IEEE Trans. Med. Imaging*, vol. 30, no. 2, pp. 295–305, Feb. 2011.

[20] L. Sandrin, M. Tanter, S. Catheline, and M. Fink, "Shear modulus imaging with 2-D transient elastography," *IEEE Trans. Ultrason. Ferroelectr. Freq. Control*, vol. 49, no. 4, pp. 426–435, 2002.

[21] M. Tanter, J. Bercoff, A. Athanasiou, T. Deffieux, J.-L. Gennisson, G. Montaldo, M. Muller, A. Tardivon, and M. Fink, "Quantitative assessment of breast lesion viscoelasticity: Initial clinical results using supersonic shear imaging," *Ultrasound Med. Biol.*, vol. 34, no. 9, pp. 1373–1386, Sep. 2008.

[22] R. H. Behler, T. C. Nichols, E. P. Merricks, and C. M. Gallippi, "Reflected shear wave imaging of atherosclerosis," in *2009 IEEE International Ultrasonics Symposium*, pp. 2445–2448.

[23] M. Palmeri, N. Rouze, M. Wang, X. Ding, and K. Nightingale, "Quantifying the impact of kernel size on the accuracy and precision of shear wave estimation," in *Proc. 2010 IEEE Ultrasonics Symp.*, 2010, pp. 13–16.

[24] A. Manduca, D. S. Lake, S. A. Kruse, and R. L. Ehman, "Spatiotemporal directional filtering for improved inversion of MR elastography images," *Med. Image Anal.*, vol. 7, no. 4, pp. 465–473, Dec. 2003.

[25] J. Bercoff, M. Tanter, M. Muller, and M. Fink, "The role of viscosity in the impulse diffraction field of elastic waves induced by the acoustic radiation force," *IEEE Trans. Ultrason. Ferroelectr. Freq. Control*, vol. 51, no. 11, pp. 1523–1536, 2004.

[26] N. C. Rouze, M. H. Wang, M. L. Palmeri, and K. R. Nightingale, "Robust estimation of time-of-flight shear wave speed using a Radon sum transformation," *IEEE Trans. Ultrason. Ferroelectr. Freq. Control*, vol. 57, no. 12, pp. 2662–2670, Dec. 2010.